

Joint denoising and HDR for RAW video sequences

A. Buades

O. Martorell

M. Sánchez-Beeckman

Abstract

We propose a patch-based method for the simultaneous denoising and fusion of a sequence of RAW multi-exposed images. A spatio-temporal criterion is used to select similar patches along the sequence, and a weighted principal component analysis permits to both denoise and fuse the multi exposed data. The overall strategy permits to denoise and fuse the set of images without the need of recovering each denoised image in the multi-exposure set, leading to a very efficient procedure. Several experiments show that the proposed method permits to obtain state-of-the-art fusion results with real RAW data.

1 Introduction

Conventional cameras are not able to capture in one shot the whole range of natural light present in a scene. As a consequence, dark or bright regions might appear completely saturated. A High Dynamic Range (HDR) image has a range of luminosity between the brightest area and the darkest area larger than usual. High Dynamic Range imaging refers to the set of methods and techniques that permit to increase the dynamic range of images and videos. Particularly, we will deal with the combination of several low dynamic range images of the same scene acquired with different exposure times, in order to create a HDR image.

Most methods combine the radiance values instead of the usual color values of standard 8 bit per pixel and channel images. In order to do so, the camera response function (CRF) has to be estimated, generally using the method proposed by Debevec and Malik [19]. When using the radiance, the result obtained by a HDR method has to be converted into a standard representation, for visualization in common displays. This process is known as tone-mapping [72]. Methods combining the usual color values are referred as Multi Exposure Fusion (MEF) methods [56] and do not need additional tone-mapping.

There exists a wide literature on HDR imaging. Many classical methods combine the set of images using a weighted average of irradiance values:

$$E(x, y) = \sum_{i=1}^N w(I_i(x, y)) \left(\frac{g^{-1}(I_i(x, y))}{t_i} \right) / \sum_{i=1}^N w(I_i(x, y)) \quad (1)$$

where I_1, \dots, I_N denote the input images, g is the camera transfer function and $w(\cdot)$ is designed to diminish the contribution of under and over exposed pixels. For computing $w(\cdot)$, the most commonly used methods are the ones proposed by Debevec and Malik [19], Mitsunaga and Nayar [59] or Mann and Picard [53]. Figure 1 displays some examples of weighting functions.

In order to apply the weighted average in Equation (1), the image sequence needs to be static, that is, the objects in the scene do not move and the camera is fixed. This is not the case for many sequences, and the application of such methods introduces ghosting effects. To avoid these artefacts, methods have to be adapted

to non-static image sequences [35, 43]. Recently, deep learning based methods have been proposed dealing implicitly with the ghosting effect as a part of the proposed network [40].

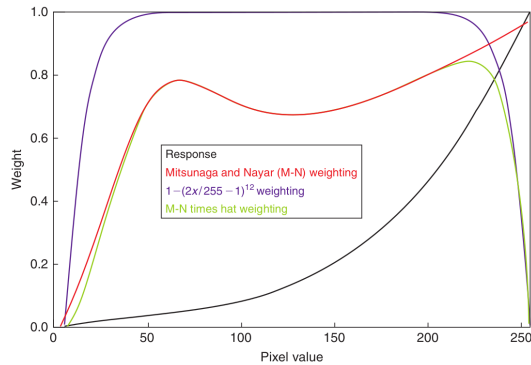


Figure 1: Several HDR weighting functions.

While the application of the inverse transfer function permits to combine values acquired with different exposure, it is not adequate for taking care of noise. Most common cameras use a CCD or CMOS sensor device measuring a single color per pixel. The selected configuration of the sensor usually follows the Bayer color filter array (CFA) [7]. Thus, out of a group of four pixels, two are green (in quincunx), one is red and one is blue [4]. Demosaicking is the interpolation process by which the two missing color values are estimated. The demosaicking is usually performed by combining close values from the same channel or the other two. As a result, the noise, being almost white at the sensor, gets color and spatial correlated. The rest of the imaging chain, consisting mainly in color and gamma corrections and compression, enhances the noise in dark parts of the image leading to contrasted colored spots of several pixels. The size of these spots depends on the applied demosaicking method. The inversion of the transfer function is not able to revert all noise correlating stages. For this reason, we will perform denoising and HDR fusion in the RAW domain.

HDR methods using the weighted average (1) actually reduce noise, but this reduction is rather minor due to the small number of values being involved. Video denoising methods take into account a spatio-temporal neighborhood of each pixel under consideration improving the noise reduction capabilities. Inspired by the video denoising method in [10] and classical HDR methods, we will propose a joint denoising and HDR method removing noise and building a HDR image free of ghosting artifacts.

The paper is organized as follows: Section 2 describes the existing literature on MEF methods. In Section 3 we describe the complete method. In Section 4, we discuss the implementation of the method and compare with state of the art algorithms.

2 Related work

2.1 Image sequence white noise removal

Local average methods, as the bilateral filter [79], or patch based methods as NL-means [9] or BM3D [17] and NLBayes [46] can be easily adapted to image sequences just by extending the neighboring area to the adjacent

frames. Kervrann and Boulanger [8] extended the NL-means to video by growing adaptively the spatio-temporal neighborhood. Arias et al. extended the NL-Bayes [46] to video [5, 6]. Methods based in sparse decompositions are extended to image sequences [52, 68, 86, 48], as well as approaches based on low rank approximation [38, 39].

The performance of many denoising methods is improved by introducing motion compensation. These compensated filters estimate explicitly the motion of the sequence and compensate the neighborhoods yielding stationary data [61]. The BM3D extension, VBM4D [51], exploits the mutual similarity between 3-D spatio-temporal volumes constructed by tracking blocks along trajectories defined by the motion vectors. In [10] the authors proposed to combine optical flow estimation and patch based methods for denoising. Their algorithm tends to a fusion of the neighboring frames in the absence of occlusions and a dense temporal sampling. In this ideal scenario, an optical flow or global registration is able to align the frames and fusion is achieved by simple averaging [30]. The algorithm in [10] compensates the failure of these requirements by introducing spatiotemporal patch comparison and denoising in an adapted PCA based transform.

Recently, neural network methods appeared making use of motion compensation [76], patch based processing [18, 83] or being applied recursively in groups of three consecutive frames [77]. Self-supervised methods have also been proposed by using warped neighboring frames to define the loss function [20].

2.2 Noise removal at the CFA and joint denoising-desaicking

Since desaicking is the main cause of noise correlation, it is suitable to remove the noise before this process, or simply combine them in a single procedure. Paliy et al. [62] performs interpolation and denoising of a single CFA Bayer image. The method uses inter color filters selected by polynomial approximation. Chatterjee et al. [15] denoises the CFA by using the NL-means algorithm. Their method averages only patches having the same CFA pattern. The authors do not use any variance stabilization transform. They propose a desaicking method based on an optimization process where the CFA is taken as the low resolution counterpart in a super resolution framework.

Zhang *et al.* [92] proposed to first denoise the CFA before applying a spatio-temporal desaicking algorithm. A spatio temporal extension of [93] is applied for denoising by combining only patches having the same CFA pattern. Noise is reduced by thresholding in an adaptive PCA basis. An initial desaicking is processed by a spatial-temporal algorithm in order to reduce artifacts. For a given pixel to be processed, one searches for the similar pixels to it within the spatial-temporal neighborhood and then let the enhanced pixel be the weighted average of them.

Heide et al. [32] proposed a single optimization process being able to deal with all image chain stages. Denoising, desaicking and deconvolution are written in a single energy minimization solved by primal-dual techniques [14]. The method applies to a single image, even it can be adapted to deal with image sequences. Patil et al. [65] denoise the CFA sensor data by a dictionary learning combined with a variance stabilization transform. No particular desaicking algorithm is proposed. Hasinoff et al. [31] proposed a chain for burst sequences of images, with the novelty of dealing with the Bayer data. The method aligns and merges all images of the burst sequence into a single one. Subsampled Bayer of factor 2 is used for alignment, a tiled translation is estimated by a Gaussian pyramid process. Finally, a robust merging method is implemented using the FFT.

Neural networks have also been recently proposed for burst fusion Mildenhall et al. [57] and joint denoising and desaicking [44].

2.3 HDR static

Classical HDR methods proposed several weight functions and CRF estimation strategies to be applied with the averaging (1). Mann and Picard [53] proposed to use as weighting function the derivative of the CRF, since greater response sensitivity corresponds to greater certainty on the irradiance values. Debevec and Malik [19] and Khan et al. [43] use both a hat function, based on the assumption that well exposed values, closer to the mid-range, are more reliable than over or under-exposed pixels. Based on signal theory, Mitsunaga and Nayar [59] propose to multiply Mann and Picard’s weight by the response output, since larger values are less influenced by a constant noise floor. Figure 1 shows some example of weighting functions for HDR fusion for static sequences.

More recent methods are proposed to perform HDR fusion by using deep learning techniques, such as classic convolutional neural networks [40] or other models, such as generative adversarial networks [60]. Although these methods aim at improving the visual quality of the result, they are more devoted to remove ghosting artefacts due to motion of the camera or objects in the scene.

2.4 HDR deghosting

Tursun et al. [82] presented a taxonomy for classification of HDR deghosting algorithms. Here we provide a summary of the proposed classification, as well as more recent methods posterior to the published taxonomy. For a more extense review, please refer to Tursun et al. article.

The proposed classification divides the methods into two groups: on one hand, methods that remove artifacts due to global camera motion (named global alignment algorithms) and methods that remove artefacts that result from moving objects in the scene (named moving object algorithms). This second family of methods usually assume that the camera is static. Both families can be combined for hand-held camera deghosting.

Global alignment algorithms aim at detecting different global motion models: translation [85, 2], rotation [13], affinity [36] or homography [54, 80]. There exist a variety of methods for estimating the desired motion model: Rad et al. [69] and Yao [91] propose to register the images by translating the problem to the Fourier domain; Mann et al. [54] and Candocia [12] use the comparametric equations to find the desired global transformation; Tomaszewska and Mantiuk [80] and Gevrekci and Gunturk [25] find the transformation by matching image descriptors, such as SIFT [50] or CIFT.

Moving object algorithms can be divided in several subclasses, depending on the main strategy used to remove ghosting artefacts: moving object removal, moving object selection or moving object registration. Moving object removal algorithms replace selected regions by an estimation of the static background. These methods may fail in presence of dynamic backgrounds, moving objects with occlusions or insufficient number of exposures [43, 66, 27, 74]. Moving object selection detects the presence of moving regions and substitute those pixels by corresponding areas from other images [28, 37, 70]. Moving object registration methods remove the majority of artefacts by computing motion between a reference frame and the other images of the stack. The methods in this family can also be classified in two subclasses: optical flow methods [33, 94, 24] or patch based methods [34, 73]. The methods in the first group aim at finding a pixel-wise motion between images, while the ones in the latter use patch-based strategies to register images and remove artefacts.

There also exist more recent methods using deep learning techniques to remove ghosting artefacts. The first method using a convolutional neural network was Kalantari et al. [40], which perform a pixel-wise merging. Wu et al. [87] propose a non-flow-based approach for HDR; Yan et al. [88] handle motion between images by an attention module and later they proposed a non-local network [89]. HDR-GAN [60] propose a novel GAN-based

model with a novel generator network. This network contains a reference-based residual merging block, which is able to align large objects and camera registration. Other artefacts are removed by a deep HDR supervision scheme. Liu et al. [49] align the dynamic frames with a deformable alignment module. They propose to use a two branch network, to process separately LDR images and irradiance images, since they provide different information about the scene.

2.5 Joint HDR and noise removal

There is very few literature of HDR imaging dealing with noise removal. Akyuz et al. [3] denoise each frame before fusion, by averaging in the radiance domain a subset of frames. Tico et al. [78] combine an initial fusion with the image of the sequence with the shortest exposure in the luminance domain. This combination is performed in the wavelet domain and coefficient attenuation is applied to the coefficients of the difference of luminances. Min et al. [58] filter the set of images by spatio-temporal motion compensated anisotropic filters prior to HDR reconstruction. Lee et al. [47] use sub-band architecture for fusion, with a weighted combination using a motion indicator function to avoid ghosting effects. The low frequency bands are filtered with a multi-resolution bilateral filter while the high frequency bands are filtered by soft thresholding. Ahmad et al. [1] identify noisy pixels and reduce their weight during image fusion. Goossens et al. [26] propose a realistic noise model for HDR imaging that takes into account an accurate noise model of image capture. With that, they modify the HDR weights to improve the PSNR. Kronander et al. [45] propose a unified framework for HDR reconstruction from raw CFA data. The proposed method is based on an adaptive spatial and cross-sensor filtering using a polynomial approximation. During reconstruction, they perform CFA interpolation, resampling and HDR assembly in a single operation.

2.6 Tone Mapping

Tone-mapping algorithms are closely related with HDR imaging since they are necessary for the visualization of HDR images in common display devices. Tone-mapping algorithms can be classified into global and local methods. Global methods apply a single tone-mapping curve on each pixel of the image [81, 84], while local methods make use of local spatial properties to perform the task adaptatively on each pixel [29]. Global methods require less computation and are faster than local ones. Durand and Dorsey [22] proposed a bilateral filter which is able to preserve edges and remove most halo artefacts. Mantiuk et al. [55] proposed a contrast processing framework. Farbman et al. [23] use a multi-scale strategy and a least-square filter to perform tone-mapping. Paris et al. [63] proposed a local Laplacian filter which increases contrast locally by applying a monotonic remapping function to the coefficients of a Laplacian pyramid.

Although classical methods for tone-mapping produce good results, hyper-parameter tuning is needed to achieve the best visual quality and reduce halo effects. To overcome these problems, deep learning-based methods were proposed: a generative adversarial network (GAN) [64], an autoencoder network with skip connections [90], conditional generative adversarial networks (cGAN) [71] or bicycleGAN [75].

3 Proposed joint HDR and noise removal method

The proposed algorithm performs a joint denoising and HDR of a reference RAW image given a series of—not necessarily static—accompanying images taken under a variety of exposure times.

3.1 Noise model with different exposure times

Let $\mathcal{I} = \{I_1, I_2, \dots, I_N\}$ be a sequence of noisy RAW images with corresponding exposure times $\{\tau_1, \tau_2, \dots, \tau_N\}$. As in [11], each one of these images is converted into a 4-channel image of half the width and height of the original RAW one, containing the red, blue and two green values. These are still denoted as I_i .

The first step we take is to estimate the level of noise that is present in each one of the four channels of the disassembled CFA. Since all images are assumed to have been taken with the same ISO value, their noise curves $\{\sigma_1, \sigma_2, \dots, \sigma_N\}$ are identical and denoted by $\sigma(x)$, depending on the color value x .

We use the same approach in [11] which adapts the single image noise estimation algorithm in [16]. This algorithm divides each image in patches and applies the DCT as proposed by Ponomarenko [67] for uniform noise estimation. The low frequencies of the DCT permit to select the less oscillating patches, and the high frequencies of these selected patches yield a standard deviation estimate.

Patches from all the initial images are classified in bins depending on its mean, which permits to estimate a standard deviation for each color, and thus an intensity dependent model. The algorithm yields a set of observations $\{x_i, \sigma(x_i)\}$ which has to be interpolated to the whole range in order to have a complete noise model. Noise at the sensor is often assumed to follow a Poisson distribution, with linear variance.

The noise estimation is applied independently for each of the four channels, leading to the estimation model $\sigma = (\sigma_r, \sigma_{g_1}, \sigma_{g_2}, \sigma_b)$.

3.2 Normalization and variance stabilization

Let $I_{\text{ref}} \in \mathcal{I}$ be chosen as reference, we perform an initial normalization step by equalizing the exposure of each image to this reference one. This is accomplished by normalizing the exposure time taking care of the black offset,

$$\hat{I}_i = O + \frac{\tau_{\text{ref}}}{\tau_i}(I_i - O), \quad (2)$$

being O the constant black offset image. The image I_{ref} is chosen to be the middle-exposed one. Due to this normalization, the noise model of each \hat{I}_i becomes

$$\bar{\sigma}_i^2(x) = \frac{\tau_{\text{ref}}^2}{\tau_i^2} \sigma^2\left(\frac{\tau_i}{\tau_{\text{ref}}} x\right) \quad \forall i \in \{1, \dots, N\}. \quad (3)$$

Given any image with signal dependent noise model $\sigma(x)$, a variance stabilization transform $f(x)$ permits to convert this image into a new one having a uniform noise variance,

$$f_k(x) = \int_0^x \frac{\sigma_0 dt}{\sigma_k(t)},$$

being σ_0 a fixed noise standard deviation and k indicates the image channel. When assuming a linear variance model, this stabilization is known as the Anscombe transform. This transformation is different for each channel, since each one has its own noise function $\sigma = (\sigma_r, \sigma_{g_1}, \sigma_{g_2}, \sigma_b)$.

We apply such a variance stabilization transform to each one of the normalized images \hat{I}_i . We use the same estimated noise curve to modify every \hat{I}_i . It can be proved that, if the noise variance is approximated linearly, the uniform variance of the stabilized images, $\hat{\sigma}_i$, differs from σ_0 by exactly a scaling factor $\sqrt{\tau_{\text{ref}}/\tau_i}$ and $\hat{\sigma}_{\text{ref}} = \sigma_0$.

The color of the variance stabilized images is comparable even if their noise standard deviation is different. We will take advantage of that in the next step, where the data from brighter, less noisy images will have a greater impact on the final result.

3.3 Joint denoising and HDR

From now on, we assume that every frame $\hat{I}_i \in \hat{\mathcal{I}}$ has a uniform noise standard deviation $\hat{\sigma}_i$, while any mention of $I_i \in \mathcal{I}$ refers to the original, pre-normalization image using the RRGB space.

We will use a decorrelation transform YUVW for each 4-channel image \hat{I}_i given by matrix

$$M = \begin{pmatrix} 0.5 & 0.5 & 0.5 & 0.5 \\ -0.5 & 0.5 & 0.5 & -0.5 \\ 0.65 & 0.2784 & -0.2784 & -0.65 \\ -0.2784 & 0.65 & -0.65 & 0.2784 \end{pmatrix}.$$

This transform was computed by applying a Principal Component Analysis (PCA) to several 4-channel images obtained from RAW. If we assume that noise values at the sensor data are uncorrelated for different color channels and pixel locations, since this is an orthonormal matrix, its application to \hat{I}_i conserves the decorrelation and uniform standard deviation properties. The transposed matrix yields the inverse transform.

Firstly, we compute the optical flow between the better exposed frame \hat{I}_{ref} and every other $\hat{I}_i \in \hat{\mathcal{I}}$ on the brightness channel Y. We check the consistency of the obtained values by also computing the inverse flows and making sure that they are approximately reciprocal. Pixels that do not verify this condition are either occluded or in violation of the optical flow’s colour constancy assumption, so we mark them as invalid for the rest of the algorithm. Then, we warp each frame onto the reference image; at this point we have a sequence of static images along with their respective occlusion masks.

Afterwards, a 3D volumetric patch-based approach is used to search for similar patches, while still 2D image patches are used for denoising and HDR synthesis. For every overlapping $k \times k$ patch in \hat{I}_{ref} , P , the patch \mathcal{P} referring to its extension to the temporal dimension is considered, having N times more pixels than the original one. Since the images have been resampled according to the estimated flow, the data is supposed to be static. The algorithm looks for the K extended patches closest to \mathcal{P} . A matrix containing the pixel values for its K most resembling extended patches of size N (i.e. a matrix of dimension $KN \times k^2$) is built.

Let P be an arbitrary patch in \hat{I}_{ref} , and \mathbf{X} the matrix whose j -th row is composed of the flattened pixel values of the 2D patch Q_j . We wish to obtain from \mathbf{X} a HDR and noise free patch. To do so, we carry out a Weighted Principal Component Analysis. For every neighbouring patch Q_j of P , we compute its associated weight

$$w_j = w_{\text{sim}}(P, Q_j) \cdot w_{\text{HDR}}(Q_j) \cdot w_{\text{SNR}}(Q_j), \quad (4)$$

where

- $w_{\text{sim}}(P, Q_j) = \exp(-\|P - Q_j\|^2 / (h \hat{\sigma}_{\text{ref}})^2)$ weights Q_j so that patches that are too dissimilar to P lose influence on the filtering step (depending on a parameter h).
- $w_{\text{HDR}}(Q_j)$ is any HDR weighting function adapted to the RAW range of intensities, evaluated on the same position and original RRGB image I_i where Q_j is located.

- $w_{\text{SNR}}(Q_j) = \sqrt{\tau_i/\tau_{\text{ref}}}$ compensates for the fact that $\hat{\sigma}_i \neq \hat{\sigma}_{\text{ref}}$, favouring patches Q_j from a frame i with a higher exposure time and thus better signal to noise ratio after normalization and variance stabilization.

The weights $\{w_j\}$ are then used to center the data in \mathbf{X} . That is, we subtract the vector

$$\mathbf{b} = \frac{1}{\sum_{j=0}^{KN} w_j} \sum_{j=0}^{KN} w_j \mathbf{x}_j$$

to each row \mathbf{x}_j of \mathbf{X} to form the centered data matrix $\bar{\mathbf{X}}$. After that, we obtain the eigendecomposition of the weighted covariance matrix

$$\frac{V_1}{V_1^2 - V_2} \bar{\mathbf{X}}^T \mathbf{W} \bar{\mathbf{X}} = \mathbf{V} \mathbf{S}^2 \mathbf{V}^T,$$

where $\mathbf{W} = \text{diag}(w_1, \dots, w_{KN})$, and V_1 and V_2 are the sum of the weights and the sum of their squares, respectively. This operation can be efficiently done by computing the SVD of $\mathbf{W}^{\frac{1}{2}} \bar{\mathbf{X}}$. The matrix $\bar{\mathbf{X}}$ is then filtered by applying a threshold on the coefficients of the PCA based on the magnitude of their associated principal values compared to the expected noise, and the patch P is subsequently reconstructed by adding back \mathbf{b} to its corresponding row in the matrix. This process is done independently for each channel and each patch on the reference frame, and an image is formed by aggregating those patches. Lastly, we apply a color space conversion back to RGB from YUVW and we undo the variance stabilizing transform to obtain the resulting image.

In particular, we note that, for noise-free images, using a window size of $k = 1$ and setting $w_{\text{sim}} = w_{\text{SNR}} = 1$ with a full cancelation of coefficients of the PCA—that is, keeping only the barycenter \mathbf{b} —is equivalent to a classic HDR procedure with weights w_{HDR} . Indeed, the vector \mathbf{b} is a spatio-temporal generalization of the classical HDR averaging with additional noise removal when using all the weight factors. The weight $w_{\text{sim}}(P, Q_j)$ permits the noise removal but also avoids creating ghosting artefacts. While the barycenter estimation would be enough to remove noise, increase dynamic range and avoid ghosting effects, texture and details might be over-smoothed. The use of PCA avoids such a detail smoothing and improves the deghosting capabilities of the method.

3.4 Imaging chain

HDR methods that are applied to common 8-bit images require a secondary step to transform the values of the radiance map that they yield to an image that can be viewed on a LDR display. This is also the case for the RAW HDR image that our algorithm outputs. However, since a radiance map and a RAW HDR image are fundamentally different, an extra set of actions need to be taken to correctly visualize the latter.

First of all, the denoised and HDR image that results from the procedure still has the structure of a 4-channel disassembled CFA. For that reason, we must reassemble it and interpolate its values into the usual red, green and blue chromatic components that can be perceived by the human eye. We accomplish this by demosaicking the image, for which we can use any state of the art method, such as [21, Section II].

After demosaicking, the signal strengths of the three colors can be somewhat unbalanced due to how the camera sensors read different types of light. Therefore, to conform them to a more realistic hue, a white balancing step is performed by multiplying each channel by a different value—chosen depending on the processed image. Moreover, to be able to visualize the image on a standard display, we apply a linear transformation to turn the camera RGB values into coordinates in the sRGB color space.

Finally, we adjust the contrast and brightness of the HDR image and compress its range so that it fits in 8 bits per channel. While a simple scaling and gamma correction is usually good enough to do so on non-HDR RAW images, we have found that more complex tone mapping algorithms [63] produce more pleasant results. Some of these algorithms have the disadvantage that they magnify image noise considerably; this is not a problem for us, given that our images have already had their noise removed.

4 Experimentation

We evaluate the HDR capability of our algorithm by testing it on sequences of real images with different exposure times and some amount of movement between frames. We study the effects of the different weights and the type of filtering in the proposed scheme.

The same parameters have been used in all experiments. We keep a fixed window size of $k = 7$, a parameter $h = 2.0$, a threshold of principal values $\tau = 2.8$. The HDR weighting function is

$$w_i(P) = 1 - \left(2 \cdot \frac{I_i(P) - O}{M - O} - 1 \right)^{12}$$

$$w_{HDR}(P) = (w_r(P) + w_{g1}(P) + w_{g2}(P) + w_b(P))/4$$

being O the black offset value, M the RAW maximum value ($M = 4095$ for current examples) and $I_i(P)$ the mean value of channel i in patch P . The resulting images are processed with Matlab’s `localtonemap` function, which implements the tone mapping algorithm in [63].

The RAW images in Figure 2 was acquired by ourselves while the images in Figures 3-4 were taken from [41, 42].

4.1 HDR in real noisy images

First, we set the method to keep none of the coefficients of the PCA, so that it only centers the patch values to those of the weighted barycenter. That way, we can study the effect each separate type of weight has on the HDR process. In particular, we notice that the introduction of patch similarity weights helps against the presence of ghosting that usually appears when applying HDR algorithms on moving images. This strong point arises from the fact that a weighting based solely on pixel intensities can mistakenly merge patches that have been aligned inaccurately; those patches give up their influence when attaching an extra weight that compares them to the reference patch. This deghosting effect is made clear in Figure 2: the translucent edges of the pen that bleed through its interior in subfigure 2b disappear completely in subfigure 2c.

We also study how the type of filtering affects both the denoising and the HDR quality. It is clear that keeping only the barycenter of each group of patches oversmooths the results, and keeping or canceling PCA coefficients based on the expected quantity of noise shows a higher level of detail. We have found that, when computing a weighted SVD, it is usually enough to keep a lower number of coefficients than in the weightless case; that is, the detail information is shifted to gather on the first few components of the PCA. In view of that, retaining PCA coefficients up to certain point adds texture without compromising the quality of the HDR. Past that point, almost only noise is added. For that reason, it can be beneficial to limit the maximum number of coefficients to keep, even if the filtering is done comparing the singular values to the noise variance, to make sure that no residual noise is accidentally preserved while also saving some computation time. Figure 3 demonstrates how our algorithm correctly denoises and expands the dynamic range of images with very dark

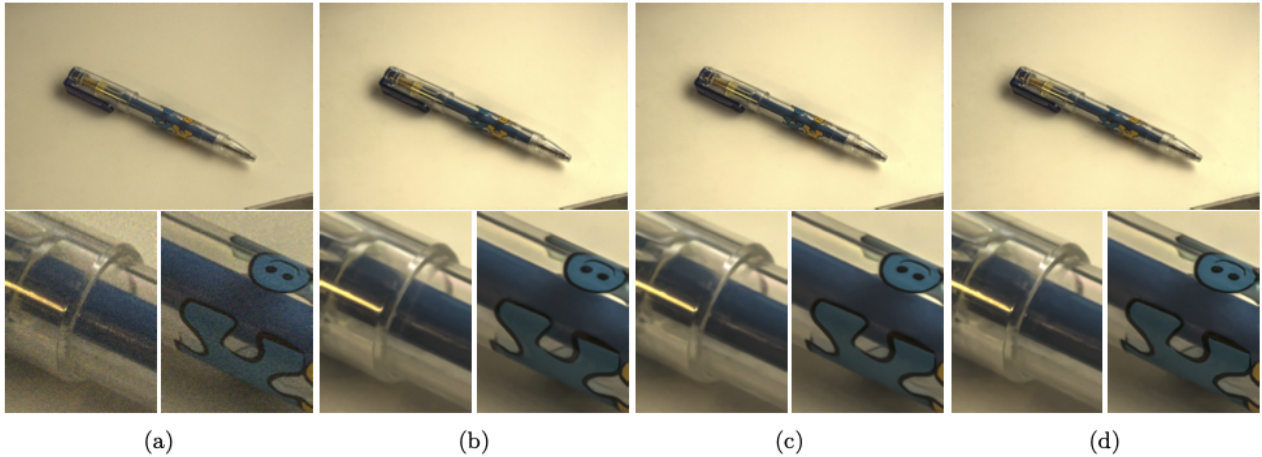


Figure 2: Ghosting effects of the HDR process are corrected with the introduction of similarity weights, and details are further improved when keeping or canceling PCA coefficients based on the noise standard deviation. (a) Tone mapped reference noisy image. (b) HDR without similarity weights (only barycenter centering). (c) HDR with similarity weights (only barycenter centering). (d) HDR with similarity weights (filtering of PCA coefficients).

and bright regions: comparing subfigures 3d, 3e and 3f, it is apparent that a small number of extra PCA coefficients are sufficient to add considerable detail to the resulting image with respect to performing a simple weighted average.

References

- [1] Attiq Ahmad, Muhammad Mohsin Riaz, Abdul Ghafoor, and Tahir Zaidi. Noise resistant fusion for multi-exposure sensors. *IEEE Sensors Journal*, 16(13):5123–5124, 2016.
- [2] Ahmet Oguz Akyüz. Photographically guided alignment for hdr images. In *Eurographics (Areas Papers)*, pages 73–74, 2011.
- [3] Ahmet Oguz Akyuz and Erik Reinhard. Noise reduction in high dynamic range imaging. *Journal of Visual Communication and Image Representation*, 18(5):366–376, 2007.
- [4] D. Alleysson, S. Susstrunk, and J. Herault. Linear demosaicing inspired by the human system. *IEEE Trans. Image Process.*, 14(4):439–449, 2005.
- [5] Pablo Arias and Jean-Michel Morel. Towards a bayesian video denoising method. In *International Conference on Advanced Concepts for Intelligent Vision Systems*, pages 107–117. Springer, 2015.
- [6] Pablo Arias and Jean-Michel Morel. Video denoising via empirical bayesian estimation of space-time patches. 2017.

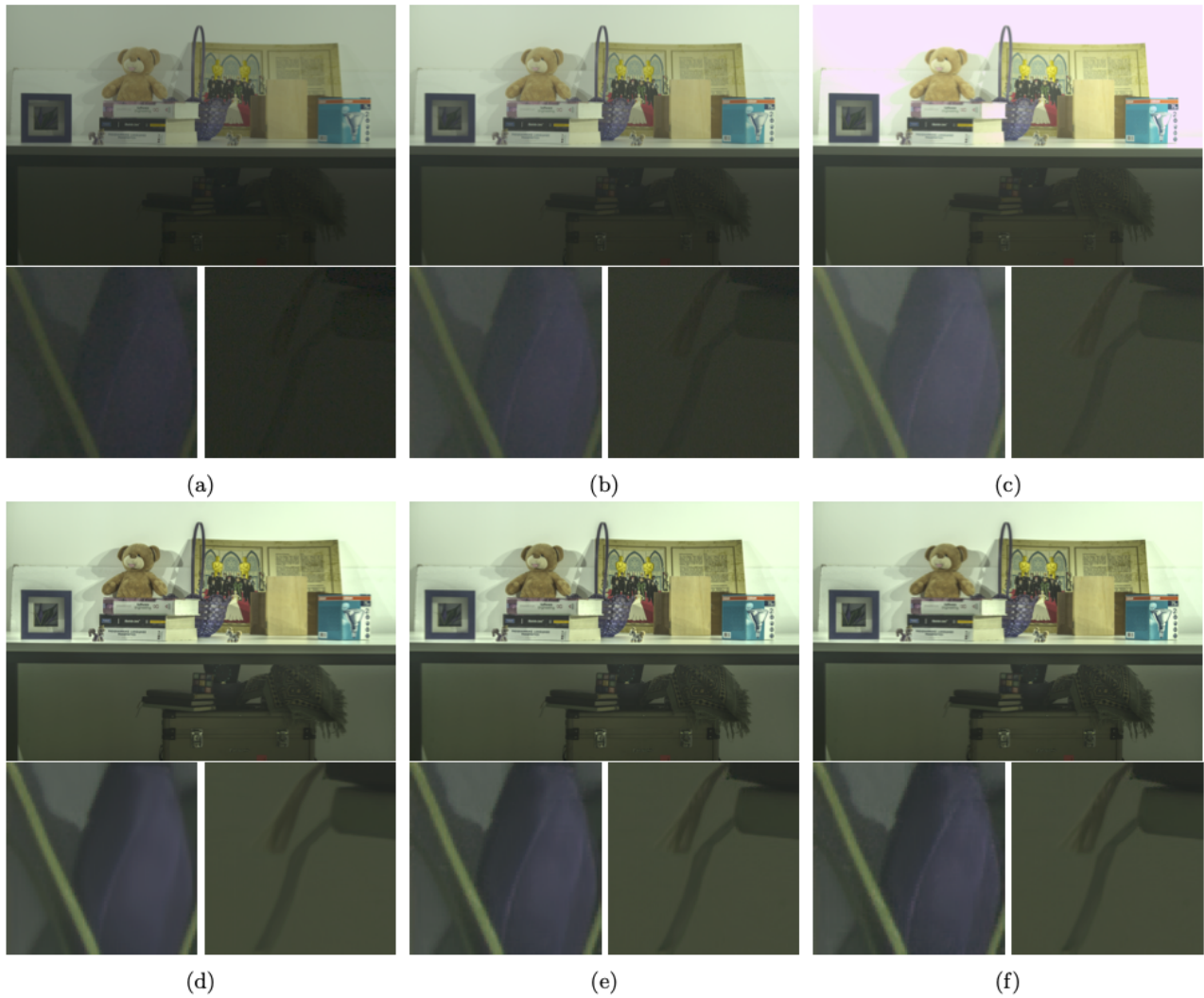


Figure 3: Weighting the PCA allows us to keep fewer coefficients without compromising too much quality. (a)–(c): original images with different exposure times. (d) HDR only with barycenter centering. (e) HDR with filtering based on noise variance (at most 3 coefficients). (f) HDR with filtering based on noise variance (no coefficient restriction).



Figure 4: Comparison of proposed scheme to classical HDR with the same HDR weighting function. Top: initial low dynamic images. Below, from left to right: classical HDR and proposed scheme.

- [7] B.E. Bayer. Color imaging array, 1976. US Patent 3 971 065.
- [8] J. Boulanger, C. Kervrann, and P. Bouthemy. Space-time adaptation for patch-based image sequence restoration. *IEEE Trans. PAMI*, 29(6):1096–1102, 2007.
- [9] A. Buades, B. Coll, and J.M. Morel. A non local algorithm for image denoising. *IEEE Computer Vision and Pattern Recognition*, 2:60–65, 2005.
- [10] A. Buades, J.L. Lisani, and M. Miladinović. Patch Based Video Denoising with Optical Flow Estimation. *IEEE Transactions on Image Processing*, 25(6):2573–2586, 2016.
- [11] Antoni Buades and Joan Duran. Cfa video denoising and demosaicking chain via spatio-temporal patch-based filtering. *IEEE Transactions on Circuits and Systems for Video Technology*, 30(11):4143–4157, 2020.
- [12] Frank M Candocia. Simultaneous homographic and comparametric alignment of multiple exposure-adjusted pictures of the same scene. *IEEE Transactions on Image Processing*, 12(12):1485–1494, 2003.
- [13] Lukas Cerman and Vaclav Hlavac. Exposure time estimation for high dynamic range imaging with hand held camera. In *Proc. of Computer Vision Winter Workshop, Czech Republic*. Citeseer, 2006.
- [14] Antonin Chambolle and Thomas Pock. A first-order primal-dual algorithm for convex problems with applications to imaging. *Journal of mathematical imaging and vision*, 40(1):120–145, 2011.
- [15] Priyam Chatterjee, Neel Joshi, Sing Bing Kang, and Yasuyuki Matsushita. Noise suppression in low-light images through joint denoising and demosaicing. In *Computer Vision and Pattern Recognition (CVPR), 2011 IEEE Conference on*, pages 321–328. IEEE, 2011.
- [16] Miguel Colom, Antoni Buades, and Jean-Michel Morel. Nonparametric noise estimation method for raw images. *JOSA A*, 31(4):863–871, 2014.

- [17] K. Dabov, A. Foi, V. Katkovnik, K. Egiazarian, et al. Bm3d image denoising with shape-adaptive principal component analysis. *Proc. of the Workshop on Signal Processing with Adaptive Sparse Structured Representations, Saint-Malo, France*, April 2009.
- [18] Axel Davy, Thibaud Ehret, Jean-Michel Morel, Pablo Arias, and Gabriele Facciolo. A non-local cnn for video denoising. In *2019 IEEE International Conference on Image Processing (ICIP)*, pages 2409–2413. IEEE, 2019.
- [19] Paul E Debevec and Jitendra Malik. Recovering high dynamic range radiance maps from photographs. In *ACM SIGGRAPH 2008 classes*, page 31. ACM, 2008.
- [20] Valéry Dewil, Jérémy Anger, Axel Davy, Thibaud Ehret, Gabriele Facciolo, and Pablo Arias. Self-supervised training for blind multi-frame video denoising. In *Proceedings of the IEEE/CVF Winter Conference on Applications of Computer Vision*, pages 2724–2734, 2021.
- [21] Joan Duran and Antoni Buades. Self-similarity and spectral correlation adaptive algorithm for color demosaicking. *IEEE transactions on image processing*, 23(9):4031–4040, 2014.
- [22] F. Durand and J. Dorsey. Fast bilateral filtering for the display of high-dynamic-range images. In *Proceedings of the 29th annual conference on Computer graphics and interactive techniques*, pages 257–266. ACM New York, NY, USA, 2002.
- [23] Zeev Farbman, Raanan Fattal, Dani Lischinski, and Richard Szeliski. Edge-preserving decompositions for multi-scale tone and detail manipulation. *ACM Transactions on Graphics (TOG)*, 27(3):1–10, 2008.
- [24] Sira Ferradans, Marcelo Bertalmío, Edoardo Provenzi, and Vicent Caselles. Generation of hdr images in non-static conditions based on gradient fusion. In Gabriela Csurka and José Braz, editors, *VISAPP (1)*, pages 31–37. SciTePress, 2012.
- [25] Murat Gevrekci and Bahadır K Gunturk. On geometric and photometric registration of images. In *2007 IEEE International Conference on Acoustics, Speech and Signal Processing-ICASSP'07*, volume 1, pages I–1261. IEEE, 2007.
- [26] Bart Goossens, Hiệp Luong, Jan Aelterman, Aleksandra Pižurica, and Wilfried Philips. Realistic camera noise modeling with application to improved hdr synthesis. *EURASIP Journal on Advances in Signal Processing*, 2012(1):1–28, 2012.
- [27] Miguel Granados, Hans-Peter Seidel, and Hendrik PA Lensch. Background estimation from non-time sequence images. In *Proceedings of graphics interface 2008*, pages 33–40, 2008.
- [28] Thorsten Grosch et al. Fast and robust high dynamic range image generation with camera and object movement. *Vision, Modeling and Visualization, RWTH Aachen*, 277284, 2006.
- [29] Bo Gu, Wujing Li, Minyun Zhu, and Minghui Wang. Local edge-preserving multiscale decomposition for high dynamic range image tone mapping. *IEEE Transactions on image Processing*, 22(1):70–79, 2012.
- [30] Gloria Haro, Antoni Buades, and Jean-Michel Morel. Photographing paintings by image fusion. *SIAM Journal on Imaging Sciences*, 5(3):1055–1087, 2012.

- [31] Samuel W Hasinoff, Dillon Sharlet, Ryan Geiss, Andrew Adams, Jonathan T Barron, Florian Kainz, Jiawen Chen, and Marc Levoy. Burst photography for high dynamic range and low-light imaging on mobile cameras. *ACM Transactions on Graphics (TOG)*, 35(6):192, 2016.
- [32] Felix Heide, Markus Steinberger, Yun-Ta Tsai, Mushfiqur Rouf, Dawid Pajak, Dikpal Reddy, Orazio Gallo, Jing Liu, Wolfgang Heidrich, Karen Egiazarian, et al. Flexisp: A flexible camera image processing framework. *ACM Transactions on Graphics (TOG)*, 33(6):231, 2014.
- [33] Imtiaz Hossain and Bahadir K Gunturk. High dynamic range imaging of non-static scenes. In *Digital Photography VII*, volume 7876, page 78760P. International Society for Optics and Photonics, 2011.
- [34] Jun Hu, Orazio Gallo, and Kari Pulli. Exposure stacks of live scenes with hand-held cameras. *Computer Vision–ECCV 2012*, pages 499–512, 2012.
- [35] Jun Hu, Orazio Gallo, Kari Pulli, and Xiaobai Sun. Hdr deghosting: How to deal with saturation? In *Proceedings of the IEEE Conference on Computer Vision and Pattern Recognition*, pages 1163–1170, 2013.
- [36] Jaehyun Im, Sangsik Jang, Seungwon Lee, and Joonki Paik. Geometrical transformation-based ghost artifacts removing for high dynamic range image. In *2011 18th IEEE International Conference on Image Processing*, pages 357–360. IEEE, 2011.
- [37] Katrien Jacobs, Celine Loscos, and Greg Ward. Automatic high-dynamic range image generation for dynamic scenes. *IEEE Computer Graphics and Applications*, 28(2):84–93, 2008.
- [38] Hui Ji, Sibin Huang, Zuowei Shen, and Yuhong Xu. Robust video restoration by joint sparse and low rank matrix approximation. *SIAM Journal on Imaging Sciences*, 4(4):1122–1142, 2011.
- [39] Hui Ji, Chaoqiang Liu, Zuowei Shen, and Yuhong Xu. Robust video denoising using low rank matrix completion. In *Computer Vision and Pattern Recognition (CVPR), 2010 IEEE Conference on*, pages 1791–1798. IEEE, 2010.
- [40] Nima Khademi Kalantari and Ravi Ramamoorthi. Deep high dynamic range imaging of dynamic scenes. *ACM Trans. Graph.*, 36(4):144–1, 2017.
- [41] Kanita Karaduzovic-Hadziabdic, Telalovic J Hasic, and Rafal Konrad Mantiuk. Multi-exposure image stacks for testing hdr deghosting methods. 2017.
- [42] Kanita Karajuzovic-Hadziabdic, Jasminka Hasic Telalovic, and Rafal K Mantiuk. Assessment of multi-exposure hdr image deghosting methods. *Computers & Graphics*, 63:1–17, 2017.
- [43] Erum Arif Khan, Ahmet Oguz Akyuz, and Erik Reinhard. Ghost removal in high dynamic range images. In *2006 International Conference on Image Processing*, pages 2005–2008. IEEE, 2006.
- [44] Filippos Kokkinos and Stamatios Lefkimmiatis. Iterative joint image demosaicking and denoising using a residual denoising network. *IEEE Transactions on Image Processing*, 28(8):4177–4188, 2019.
- [45] Joel Kronander, Stefan Gustavson, Gerhard Bonnet, and Jonas Unger. Unified hdr reconstruction from raw cfa data. In *IEEE international conference on computational photography (ICCP)*, pages 1–9. IEEE, 2013.

- [46] M. Lebrun, A. Buades, and J.-M. Morel. A nonlocal bayesian image denoising algorithm. *SIAM Journal on Imaging Sciences*, 6(3):1665–1688, 2013.
- [47] Dong-Kyu Lee, Rae-Hong Park, and Soonkeun Chang. Ghost and noise removal in exposure fusion for high dynamic range imaging. *International Journal of Computer Graphics & Animation*, 4(4):1, 2014.
- [48] Hwea Yee Lee, Wai Lam Hoo, and Chee Seng Chan. Color video denoising using epitome and sparse coding. *Expert Systems with Applications*, 42(2):751–759, 2015.
- [49] Zhen Liu, Wenjie Lin, Xinpeng Li, Qing Rao, Ting Jiang, Mingyan Han, Haoqiang Fan, Jian Sun, and Shuaicheng Liu. Adnet: Attention-guided deformable convolutional network for high dynamic range imaging. In *Proceedings of the IEEE/CVF Conference on Computer Vision and Pattern Recognition*, pages 463–470, 2021.
- [50] G Lowe. Sift-the scale invariant feature transform. *Int. J.*, 2(91-110):2, 2004.
- [51] M. Maggioni, G. Boracchi, A. Foi, and K. Egiazarian. Video denoising using separable 4D nonlocal spatiotemporal transforms. In *IS&T/SPIE Electronic Imaging*, pages 787003–787003. International Society for Optics and Photonics, 2011.
- [52] J. Mairal, G. Sapiro, and M. Elad. Learning multiscale sparse representations for image and video restoration. *SIAM Multiscale Modeling and Simulation*, 7(1):214–241, 2008.
- [53] S Mann and R Picard. Beingundigital’with digital cameras. *MIT Media Lab Perceptual*, 1:2, 1994.
- [54] Steve Mann, Corey Manders, and James Fung. Painting with looks: Photographic images from video using quantimetric processing. In *Proceedings of the tenth ACM international conference on Multimedia*, pages 117–126, 2002.
- [55] Rafal Mantiuk, Karol Myszkowski, and Hans-Peter Seidel. A perceptual framework for contrast processing of high dynamic range images. *ACM Transactions on Applied Perception (TAP)*, 3(3):286–308, 2006.
- [56] Tom Mertens, Jan Kautz, and Frank Van Reeth. Exposure fusion. In *Proceedings of the 15th Pacific Conference on Computer Graphics and Applications*, PG '07, pages 382–390, Washington, DC, USA, 2007. IEEE Computer Society.
- [57] Ben Mildenhall, Jonathan T Barron, Jiawen Chen, Dillon Sharlet, Ren Ng, and Robert Carroll. Burst denoising with kernel prediction networks. *arXiv preprint arXiv:1712.02327*, 2017.
- [58] Tae-Hong Min, Rae-Hong Park, and SoonKeun Chang. Noise reduction in high dynamic range images. *Signal, Image and Video Processing*, 5(3):315–328, 2011.
- [59] Tomoo Mitsunaga and Shree K Nayar. Radiometric self calibration. In *Proceedings. 1999 IEEE computer society conference on computer vision and pattern recognition (Cat. No PR00149)*, volume 1, pages 374–380. IEEE, 1999.
- [60] Yuzhen Niu, Jianbin Wu, Wenxi Liu, Wenzhong Guo, and Rynson WH Lau. Hdr-gan: Hdr image reconstruction from multi-exposed ldr images with large motions. *IEEE Transactions on Image Processing*, 30:3885–3896, 2021.

- [61] M.K. Ozkan, M.I. Sezan, and A.M. Tekalp. Adaptive motion-compensated filtering of noisy image sequences. *IEEE transactions on circuits and systems for video technology*, 3(4):277–290, 1993.
- [62] Dmitriy Paliy, Alessandro Foi, Radu Bilcu, and Vladimir Katkovnik. Denoising and interpolation of noisy bayer data with adaptive cross-color filters. In *Visual Communications and Image Processing 2008*, volume 6822, page 68221K. International Society for Optics and Photonics, 2008.
- [63] Sylvain Paris, Samuel W Hasinoff, and Jan Kautz. Local laplacian filters: Edge-aware image processing with a laplacian pyramid. *ACM Trans. Graph.*, 30(4):68, 2011.
- [64] Vaibhav Amit Patel, Purvik Shah, and Shanmuganathan Raman. A generative adversarial network for tone mapping hdr images. In *National Conference on Computer Vision, Pattern Recognition, Image Processing, and Graphics*, pages 220–231. Springer, 2017.
- [65] Sukanya Patil and Ajit Rajwade. Poisson noise removal for image demosaicing. In *BMVC*, 2016.
- [66] Matteo Pedone and Janne Heikkilä. Constrain propagation for ghost removal in high dynamic range images. In *VISAPP (1)*, pages 36–41, 2008.
- [67] N. N. Ponomarenko, V. V. Lukin, M. S. Zriakhov, A. Kaarna, and J. T. Astola. An automatic approach to lossy compression of AVIRIS images. *IEEE International Geoscience and Remote Sensing Symposium*, 2007.
- [68] Matan Protter and Michael Elad. Image sequence denoising via sparse and redundant representations. *IEEE Transactions on Image Processing*, 18(1):27–35, 2009.
- [69] Ali Ajdari Rad, Laurence Meylan, Patrick Vandewalle, and Sabine Süssstrunk. Multidimensional image enhancement from a set of unregistered differently exposed images. In *Computational Imaging V*, volume 6498, page 649808. International Society for Optics and Photonics, 2007.
- [70] Shanmuganathan Raman, Vishal Kumar, and Subhasis Chaudhuri. Blind de-ghosting for automatic multi-exposure compositing. In *ACM SIGGRAPH ASIA 2009 Posters*, pages 1–1. 2009.
- [71] Aakanksha Rana, Praveer Singh, Giuseppe Valenzise, Frederic Dufaux, Nikos Komodakis, and Aljosa Smolic. Deep tone mapping operator for high dynamic range images. *IEEE Transactions on Image Processing*, 29:1285–1298, 2019.
- [72] Erik Reinhard, Greg Ward, Sumanta Pattanaik, and Paul Debevec. *High Dynamic Range Imaging: Acquisition, Display, and Image-Based Lighting (The Morgan Kaufmann Series in Computer Graphics)*. Morgan Kaufmann Publishers Inc., San Francisco, CA, USA, 2005.
- [73] Pradeep Sen, Nima Khademi Kalantari, Maziar Yaesoubi, Soheil Darabi, Dan B Goldman, and Eli Shechtman. Robust patch-based hdr reconstruction of dynamic scenes. *ACM Trans. Graph.*, 31(6):203–1, 2012.
- [74] Simon Silk and Jochen Lang. Fast high dynamic range image deghosting for arbitrary scene motion. In *Proceedings of Graphics Interface 2012*, pages 85–92. 2012.
- [75] Chien-Chuan Su, Ren Wang, Hung-Jin Lin, Yu-Lun Liu, Chia-Ping Chen, Yu-Lin Chang, and Soo-Chang Pei. Explorable tone mapping operators. In *2020 25th International Conference on Pattern Recognition (ICPR)*, pages 10320–10326. IEEE, 2021.

- [76] Matias Tassano, Julie Delon, and Thomas Veit. Dvdnet: A fast network for deep video denoising. In *2019 IEEE International Conference on Image Processing (ICIP)*, pages 1805–1809. IEEE, 2019.
- [77] Matias Tassano, Julie Delon, and Thomas Veit. Fastdvdnet: Towards real-time deep video denoising without flow estimation. In *Proceedings of the IEEE/CVF Conference on Computer Vision and Pattern Recognition*, pages 1354–1363, 2020.
- [78] Marius Tico, Natasha Gelfand, and Kari Pulli. Motion-blur-free exposure fusion. In *Image Processing (ICIP), 2010 17th IEEE International Conference on*, pages 3321–3324. IEEE, 2010.
- [79] Carlo Tomasi and Roberto Manduchi. Bilateral filtering for gray and color images. In *Computer Vision, 1998. Sixth International Conference on*, pages 839–846. IEEE, 1998.
- [80] Anna Tomaszewska and Radoslaw Mantiuk. Image registration for multi-exposure high dynamic range image acquisition. 2007.
- [81] Jack Tumblin and Holly Rushmeier. Tone reproduction for realistic images. *IEEE Computer graphics and Applications*, 13(6):42–48, 1993.
- [82] Okan Tarhan Tursun, Ahmet Oguz Akyuz, Aykut Erdem, and Erkut Erdem. The state of the art in hdr deghosting: a survey and evaluation. In *Computer Graphics Forum*, volume 34, pages 683–707. Wiley Online Library, 2015.
- [83] Gregory Vaksman, Michael Elad, and Peyman Milanfar. Patch craft: Video denoising by deep modeling and patch matching. *arXiv preprint arXiv:2103.13767*, 2021.
- [84] Greg Ward. A contrast-based scalefactor for luminance display. *Graphics Gems*, 4:415–21, 1994.
- [85] Greg Ward. Fast, robust image registration for compositing high dynamic range photographs from hand-held exposures. *Journal of graphics tools*, 8(2):17–30, 2003.
- [86] Bihan Wen, Saiprasad Ravishankar, and Yoram Bresler. Video denoising by online 3d sparsifying transform learning. In *Image Processing (ICIP), 2015 IEEE International Conference on*, pages 118–122. IEEE, 2015.
- [87] Shangzhe Wu, Jiarui Xu, Yu-Wing Tai, and Chi-Keung Tang. Deep high dynamic range imaging with large foreground motions. In *Proceedings of the European Conference on Computer Vision (ECCV)*, pages 117–132, 2018.
- [88] Qingsen Yan, Dong Gong, Qinfeng Shi, Anton van den Hengel, Chunhua Shen, Ian Reid, and Yanning Zhang. Attention-guided network for ghost-free high dynamic range imaging. In *Proceedings of the IEEE/CVF Conference on Computer Vision and Pattern Recognition*, pages 1751–1760, 2019.
- [89] Qingsen Yan, Lei Zhang, Yu Liu, Yu Zhu, Jinqiu Sun, Qinfeng Shi, and Yanning Zhang. Deep hdr imaging via a non-local network. *IEEE Transactions on Image Processing*, 29:4308–4322, 2020.
- [90] Xin Yang, Ke Xu, Yibing Song, Qiang Zhang, Xiaopeng Wei, and Rynson WH Lau. Image correction via deep reciprocating hdr transformation. In *Proceedings of the IEEE Conference on Computer Vision and Pattern Recognition*, pages 1798–1807, 2018.

- [91] Susu Yao. Robust image registration for multiple exposure high dynamic range image synthesis. In *Image Processing: Algorithms and Systems IX*, volume 7870, page 78700Q. International Society for Optics and Photonics, 2011.
- [92] Lei Zhang, Weisheng Dong, Xiaolin Wu, and Guangming Shi. Spatial-temporal color video reconstruction from noisy cfa sequence. *IEEE transactions on circuits and systems for video technology*, 20(6):838–847, 2010.
- [93] Lei Zhang, Weisheng Dong, David Zhang, and Guangming Shi. Two-stage image denoising by principal component analysis with local pixel grouping. *Pattern Recognition*, 43(4):1531–1549, 2010.
- [94] Henning Zimmer, Andrés Bruhn, and Joachim Weickert. Freehand hdr imaging of moving scenes with simultaneous resolution enhancement. In *Computer Graphics Forum*, volume 30, pages 405–414. Wiley Online Library, 2011.